Increase in Strength of Partially Stabilized Zirconia After Shot Peening

Koji TAKAHASHI[a], Kae IWANAKA[a,*] ,Toshio OSADA[b], Hitonobu KOIKE[a] ,

[a]*Yokohama National University, 79-5 Tokiwadai, Hodogaya, Yokohama 240-8501, Japan*

[b]*National Institute for Materials Science, 1-2-1 Sengen, Tukuba 305-0047, Japan*

Correspondence:

Prof. Koji Takahashi

Professor, Faculty of Engineering,

Yokohama National University,

79-5, Tokiwadai, Hodogaya, Yokohama, 240-8501, Japan.

E-mail: ktaka@ynu.ac.jp

Abstract

The effects of shot peening (SP) on the strength of partially stabilized zirconia (PSZ) were studied. The compressive residual stress, apparent fracture toughness (K_C), and bending strength values of specimens subjected to SP were investigated. Results of X-ray diffraction analyses showed that SP introduced large compressive residual stress in specimens. As a result, the K_C and bending strength values of specimens having semi-elliptical pre-cracks on their surfaces increased significantly. Shot-peened specimens having surface pre-cracks with lengths less than 140 μm exhibited strength comparable to that of smooth specimens, and fractured outside the pre-crack zone, indicating that the pre-cracks were rendered harmless by SP. Thus, the introduction of a compressive residual stress by SP is an effective technique for increasing the strength of PSZ.

Keywords: partially stabilized zirconia, shot peening, residual stress, bending strength

1. Introduction

Zirconia (ZrO_2) is a ceramic material with excellent mechanical properties. The fracture toughness of partially stabilized zirconia (PSZ) is higher than that of other ceramics, owing to transformation toughening whereby the tetragonal phase transforms to a stable monoclinic phase under stress [1]. Therefore, PSZ has been used for structural and medical applications, including cutting tools, bearings, valves, artificial bones and artificial joints. In these ceramic components, machining is an important process in the creation of the final product. However, the fracture toughness of PSZ (5−10 MPa $m^{1/2}$) is still lower than that of metallic materials. As a result, surface cracks are introduced by machining. These cracks significantly decrease the strength and the reliability of the ceramic components. In this paper, we attempt to overcome this problem by applying shot peening (SP) to PSZ.

SP is a common surface modification procedure used to increase the near-surface strength of metals [2]. Compressive residual stress is generated by the localized plastic deformation of the surface layer. SP can increase the fatigue strength of metals because the compressive residual stress prevents fatigue crack initiation and propagation [3-5]. Takahashi et al. carried out bending fatigue tests using high strength steel specimens containing surface cracks subjected to SP, and reported that a surface crack that reduced the fatigue limit by 50% could be rendered harmless by SP [3]. Fernández-Pariente reported that SP was able to improve the fatigue strength of low-alloy steel specimens with pre-existent defects, regardless of the defect type [4]. Sakamoto et al. investigated the effect of a surface flaw introduced after SP on the fatigue strength in medium carbon steel, and reported that the fatigue crack initiation life, fatigue crack growth life, and fatigue limit in the steel could all be increased by SP [5].

If surface cracks on structural parts can be rendered harmless through the use of the SP technique, the SP surface treatment will be a promising technique for increasing the reliability of PSZ and other ceramics. On the other hand, researchers believed that strengthening ceramics with SP would be difficult because cracks occur on a ceramic surface when SP is too strong. However, recent studies showed that the near-surface strength of ceramics could be improved by SP [6-10]. It has been reported that compressive residual stress could be introduced by SP or sandblasting near the surface in silicon nitride (Si_3N_4) [6,7], alumina (Al_2O_3) [7], Si_3N_4/SiC composite [8], yttria stabilized tetragonal zirconia (Y-TZP) [9], and PSZ [10]. Kosmac et al. reported that sandblasting increased bending strength of Y-TZP approximately 22% [9]. Ito et al. reported that compressive residual stress ranging from 250 to 340 MPa was introduced in the near surface of PSZ, and bending strength was increased 9% by soft SP using aluminum particles [10]. However, the effects of SP on the bending strength of PSZ containing a surface crack have not yet been studied.

The objective of this study was to investigate the effects of SP on the bending strength of PSZ containing a surface crack. Specimens containing surface cracks were subjected to SP, and the effects of SP on bending strength were investigated. The size of surface cracks that can be rendered

harmless by SP was investigated in terms of bending strength.

2. Materials and Methods

2.1 Specimen preparation

The PSZ ceramic (ZR-1, Japan Fine Ceramic Center) used in this study was commercial 3mol% Y_2O_3 partially stabilized zirconia. The Vickers hardness (HV) and density of the PSZ was 1300HV and 6.1 g/cm^3, respectively. The specimens for the bending test were machined from a PSZ rectangular plate of 5 × 50 × 80 mm^3. The dimensions of the specimens were 3 × 4 × 20 mm^3. One face of the specimens was polished to a mirror-like finish. These specimens are hereafter referred to as the "Smooth" specimens.

2.2 Shot peening and residual stress

SP was performed on the surfaces of the specimens using a direct-pressure peening system. Commercial ZrO_2 beads with a diameter of 180 μm and Vickers hardness of 1150 HV were used as the shot material. The SP conditions are listed in Table 1. The average surface roughness of the Smooth and SP specimens were 0.36 μm and 0.47 μm, respectively. The residual stresses on the surfaces of the Smooth and SP specimens were measured using the X-ray diffraction (XRD) method. Conditions for the XRD analyses are shown in Table 2 [11]. For the measurement of residual stress, bending test specimen was used. The in-depth residual stress distributions of the samples were investigated after removing the surface layers by polishing the specimens with diamond abrasive pastes of 9.0, 3.0, and 0.5 μm. The residual stress in axial direction at a center part of the polished surface was measured at each layer successively. Number of measurement point at each layer was one. We confirmed that the removal of the surface layers resulted in negligible residual stress, as mentioned in section 3.1.

2.3 Measurement of apparent fracture toughness

Smooth and SP specimens were prepared for measurement of the apparent fracture toughness (K_C) at the subsurface level. The K_C value was evaluated by the indentation fracture method, in which K_C is estimated using the following equation in accordance with the Japan Industry Standards [12]:

$$K_C = 0.026 E^{1/2} P^{1/2} \frac{a}{c^{3/2}} \quad (1)$$

where E is the Young's modulus, P is the indentation load, a is half the diagonal length of the indentation, and c is half the surface crack length ($2c$). Vickers indentations were made on the polished surfaces of the specimens by applying an indentation load of 49 N for 20 s. The Young's modulus of the tested material was 214 GPa.

2.4 Crystal structure analysis

The phase transformation induced by SP was evaluated by XRD analysis, which was performed using CuKα radiation. The scanning angle was 25–65°, and the scan speed was 2°/min. The shot pressures were set to 0.2, 0.4, and 0.6 MPa for the crystal structure analysis.

2.5 Bending test and observation

To measure the bending strength (σ_B), four types of specimens were prepared. A Vickers indentation was made on the centers of the polished faces of the Smooth specimens at loads of 4.9–98 N. These specimens are called the "Pre-cracked" specimens. We then performed SP on the surfaces of the Smooth and Pre-cracked specimens. The SP conditions are listed in Table 1. These specimens are called the "Smooth+SP" and "Pre-crack+SP" specimens, respectively. The σ_B values were determined by the three-point bending test; the span length for the test was 16 mm, as shown in Fig. 1. The bending test was performed at a cross-head speed of 0.5 mm/min at room temperature in air. The origins of the fracture were observed using optical microscopy and scanning electron microscopy (SEM).

3. Results and discussion

3.1 Residual stress owing to shot peening

Figure 2 shows the residual stress distributions of the various samples along the depth direction. The compressive residual stress on the surface of the PSZ specimen was 1400 MPa, and it reached a maximum of 1800 MPa at a depth of 20 μm. With further increases in depth, stress decreased. The residual stresses of Smooth (Non-SP) specimens before and after polishing 20 μm were indicated by solid squares in Fig.2. Compering these residual stresses, we confirmed that the removal of the surface layers by mechanical polishing resulted in negligible residual stress. Ito et al. reported that compressive residual stress ranging from 250–340 MPa was introduced near the surface of PSZ by soft SP using aluminum particles [10]. The value of compressive residual stress induced in the present study was much higher than that reported by Ito et al.. This was because the Vickers hardness of the shot material used in the present study was higher than that used in Ito's study [10].

For further comparison, the residual stress value of an Al_2O_3/SiC composite [13] and Si_3N_4 [14], both subjected to SP, are also shown. After the specimens had been subjected to SP, a large compressive residual stress was introduced on the surface of the PSZ specimen, while the residual stresses in the Al_2O_3/SiC composite and Si_3N_4 specimens were small. The compressive residual stress on the surface of the PSZ specimen was approximately two to three times higher than those on the surfaces of the Al_2O_3/SiC composite and Si_3N_4 specimens. Therefore, it was confirmed that a compressive residual stress was efficiently introduced into the PSZ specimen.

3.2 Apparent fracture toughness

Figure 3 shows the effect of SP on the apparent fracture toughness (K_C) values of the various

specimens. The K_C value of the SP specimen was 16.0 MPa•m$^{1/2}$; this value was 258% higher than the K_C value for the Smooth specimen, which was 4.5 MPa•m$^{1/2}$. The surface crack length ($2c$) of the SP specimen was smaller than that of the Smooth test specimen, as shown in Fig. 4. Further, K_C value increased with a decrease in crack length. Thus, the improvement in the K_C value due to SP can be considered to have resulted from the compressive residual stress induced by SP, which suppressed the initiation and propagation of surface cracks.

3.3 Crystal structure

Figure 5 shows the XRD profiles of the Smooth and SP specimens subjected to SP at pressures of 0.2, 0.4, and 0.6 MPa. The XRD measurements were performed after polishing the specimens to a depth of 20 μm. This was done because the surface roughness of the specimens increased slightly after they were subjected to SP, making it difficult to identify minute peaks. A monoclinic (2 1 1) peak was confirmed in the vicinity of 45° for all specimens. The monoclinic weight fractions (X_m) under the different shot pressures were calculated using Equation (2) [11]:

$$X_m = \frac{I_m(211)}{I_m(211) + I_t(011)} \tag{2}$$

where I_m(2 1 1) and I_t(0 1 1) are the integrated intensities of the (2 1 1) and (0 1 1) peaks, respectively. Table 3 shows the half-width of the tetragonal $(0\ 0\ 1)_t$ peak. The half-width increased with an increase in shot pressure. This was because the crystal spacing changed owing to the local plastic deformation introduced by SP. The monoclinic weight fraction increased significantly with the increase in shot pressure, as shown in Table 3. This was attributable to the stress-induced transformation of the tetragonal phase in the PSZ to a monoclinic one, owing to the collision of the projection materials because of SP.

The compressive residual stress induced by SP in PSZ was greater than that induced in the compared materials, as described above. The Young's modulus of the PSZ is 214 GPa; this value is smaller than those of the compared materials, which are 389 GPa [13] for the Al_2O_3/SiC composite, and 294 GPa [14] for Si_3N_4. Thus, it is believed that the large compressive residual stress in PSZ was derived from the fact that the plastic deformation and stress-induced transformation caused by SP in PSZ were greater in degree than those induced in the compared materials.

3.4 Effect of SP on bending strength

Figure 6 shows the results of the bending test for each specimen. The bending strength (σ_B) of the Pre-cracked specimens decreased significantly with an increase in pre-crack length. The σ_B value of the Pre-cracked specimen improved significantly after SP. In particular, the bending strengths of the Pre-crack+SP specimens with crack lengths of approximately 140 μm or less were comparable to those of the Smooth+SP specimens. Figures 7(a) and (b) show optical micrographs of the surface of a Pre-crack+SP specimen. The Pre-cracked specimen with a crack length of 261 μm had fractures in the pre-crack zone,

as shown in Fig. 7(a). However, most of the Pre-crack+SP specimens with crack lengths of approximately 140 μm and lower had fractured outside the pre-crack zone, as shown in Fig. 7(b) and 7(c). Figures 8(a) and (b) show SEM images of the fracture surfaces of the Pre-cracked and Pre-crack+SP specimens, respectively. The Pre-cracked specimen fractured in the pre-cracked area, as shown in Fig. 8(a). However, Pre-crack+SP specimens with a crack length of less than 140 μm fractured outside the pre-cracked area, as shown by the arrow in Fig. 8(b) and 8(c).

These results indicate that the fracture mechanism of the Pre-crack+SP specimens with crack lengths less than 140 μm was similar to that of the Smooth specimens. Therefore, surface cracks with lengths of 140 μm and lower were rendered harmless by SP. It has been reported that the compressive residual stress introduced by SP is effective in preventing the propagation of fatigue cracks in metallic materials, or in rendering them harmless [3]. As with case metals, compressive residual stress induced on the surface of PSZ reduced the effective stress intensity factor at the pre-crack tips when a bending stress load was applied. As a result, the bending strength of the Pre-crack+SP specimens was improved significantly, while pre-cracks with lengths of approximately 140 μm and less were rendered harmless. Thus, the introduction of a compressive residual stress by SP is an effective technique for increasing the strength of PSZ.

4. Conclusions

The effects of SP on the bending strength (σ_B) of a PSZ, were investigated. The primary results can be summarized as follows:

(1) The compressive residual stress induced by SP was 1400 MPa on the surface, while it reached a maximum of 1800 MPa at a depth of 20 μm. Thus, a large compressive residual stress was introduced by SP.

(2) The K_C value at the surface of the specimens subjected to SP was 258% higher than that of the Smooth specimens. The improvement in the K_C value was considered to be attributable to the compressive residual stress induced by SP.

(3) The phase transformation induced by SP was evaluated by XRD analysis. The results showed that SP induced a phase transformation from the tetragonal to the monoclinic phase.

(4) The σ_B values of the pre-cracked specimens were significantly improved by SP. Shot-peened specimens with surface cracks whose lengths were less than 140 μm fractured outside the pre-crack zone. This result indicates that the pre-cracks were rendered harmless by SP.

Acknowledgments

The authors would like to thank Prof. S. Mitsushima, Yokohama National University, and Dr. S. Saito, NHK Spring Co., Ltd., for their assistance with the XRD measurements.

References

1. Garvie RC, Hannink RH, Pascoe RT. Ceramic steel? Nature 1975;258:703–4.
2. Suresh S. Fatigue of Materials. Cambridge University Press; 1991, p. 134–5.

3. Takahashi K, Amano T, Ando K, Takahashi F. Improvement of fatigue limit by shot peening for high-strength steel containing a crack-like surface defect. Int. J Structural Integr 2011;2:281–92.
4. Fernández-Pariente I, Bagherifard S, Guagliano M, Ghelichi R. Fatigue behavior of nitride and shot peened steel with artificial small surface defects. Engineering Fracture Mechanics 2013;103:2-9
5. Sakamoto J, Lee Y, Cheong S. Effect of surface flaw on fatigue strength of shot-peened medium-carbon steel. Engineering Fracture Mechanics 2014;133:99-111.
6. Pfeiffer W, Frey T. Strengthening of ceramics by shot peening. J Eur Ceram Soc 2006;26:2639–45.
7. Moon WJ, Ito T, Uchimura S, Saka H. Toughening of ceramics by dislocation sub-boundaries. Mater Sci Eng A 2004;387–389:837–9.
8. Takahashi K, Nishio Y, Kimura Y, Ando K. Improvement of strength and reliability of ceramics by shot peening and crack-healing. J Eur Ceram Soc. 2010;30:3047–52.
9. Kosmac T, Oblak C, Jevnikar P, Funduk N, Marion L. The effect of surface grinding and sandblasting on flexural strength and reliability of Y-TZP zirconia ceramic. *Dental Materials*,1999;15:426-433
10. Itou Y, Suyama S, Huse T. Effect of soft shot peening on bending strength of partially stabilized zirconia. *Journal of the Ceramic Society of Japan*, 2003;111: 776-780 (in Japanese).
11. Tanaka K, Kurimura T, Akiniwa Y, Suzuki K, Nakamura H. X-ray residual stress measurement of yttria-partially stabilized zirconia. Trans Jpn Soc Mech Eng Ser. A, 1989;55:318–25.
12. Japan Industrial Standards R1607. Testing Method for Fracture Toughness of Fine Ceramics. Japan Standards Association, 1995.
13. Oki T, Yamamoto H, Osada T, Takahashi K. Improvement of the contact strength of Al_2O_3/SiC by a combination of shot peening and crack-healing. J Powder Techno 2013;946984.
14. Yamamoto H, Oki T, Takahashi K, Osada T. Improvement of rolling contact fatigue strength of silicon nitride by shot-peening. Trans Jpn Soc Mech Eng Ser.A, 2013;79:740–44.

Table captions

Table 1. Shot peening conditions

Table 2. Conditions for the X-ray diffraction analyses

Table 3. Half-width of $(0\ 0\ 1)_t$, monoclinic weight fraction, and integrated intensity for the different shot pressures

Figure Captions

Fig. 1. Schematic drawing of the three-point loading system, test specimen size, and machining configuration.

Fig. 2. Relationship between residual stress and depth from surface.

Fig. 3. K_C values of the different surface-treated specimens. The error bar indicates the standard deviation.

Fig. 4. Photographs of Vickers indentations and cracks in the (a) Non-SP, and (b) SP specimens.

Fig. 5. XRD pattern of the surface of a peened PSZ specimen.

Fig. 6. Relationship between bending strength and crack length.

Fig. 7. Surface of a Pre-crack+SP specimen after the bending test; bending strengths and crack lengths of (a) σ_B =1100 MPa and $2c$ = 140 μm, (b) σ_B =651 MPa and $2c$ = 261 μm, and (c) σ_B =1431 MPa and $2c$ = 52 μm.

Fig. 8. SEM images showing the origins of fractures: (a) Pre-cracked specimen, 2c = 120 μm, σ_B =354 MPa, (b) Pre-crack+SP specimens, 2c = 140 μm, σ_B =1100 MPa, and (c) Pre-crack+SP specimens, 2c = 51 μm, σ_B =1250 MPa.

Table 1 Shot peening condition

Shot system	Direct pressure system
Shot material	ZrO_2 beads (1150HV)
Shot diameter	Φ180 μm
Shot pressure	0.2 MPa
Time	30 sec
Coverage	300 %

Table 2 Conditions for X-ray diffraction analyses

Characteristic X-ray	Cu $K\alpha_1$
X-ray tube	Cu
Diffraction plane	ZrO_2 (0 2 6)
Diffraction angle	140.48°
Tube voltage	40 kV
Tube current	30 mA

Table 3 Half width $(0\ 0\ 1)_t$, monoclinic weight fraction, and integrated intensity for the different shot pressures.

Shot pressure [MPa]	Half width $(0\ 0\ 1)_t$ [deg]	I_m [cps・deg]	I_t [cps・deg]	X_m [%]
Non-SP	0.2403	-	131962	0.0
0.2	0.5053	6439	109180	5.6
0.4	0.5657	12045	127050	8.7
0.6	0.6278	11679	110090	9.6

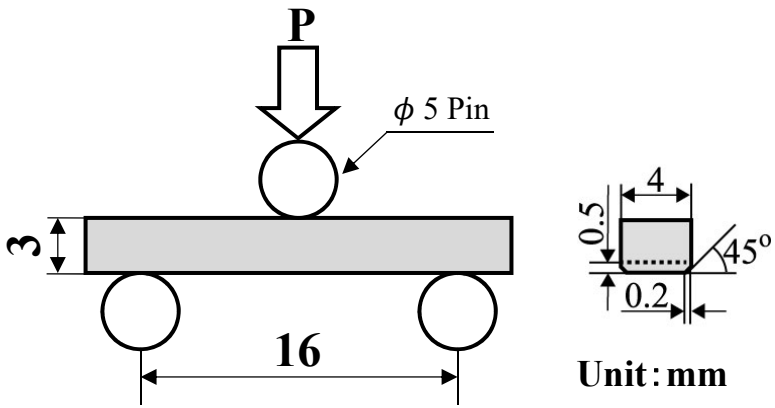

Fig. 1 Schematic drawing of the three-point loading system, test specimen size, and machining configuration.

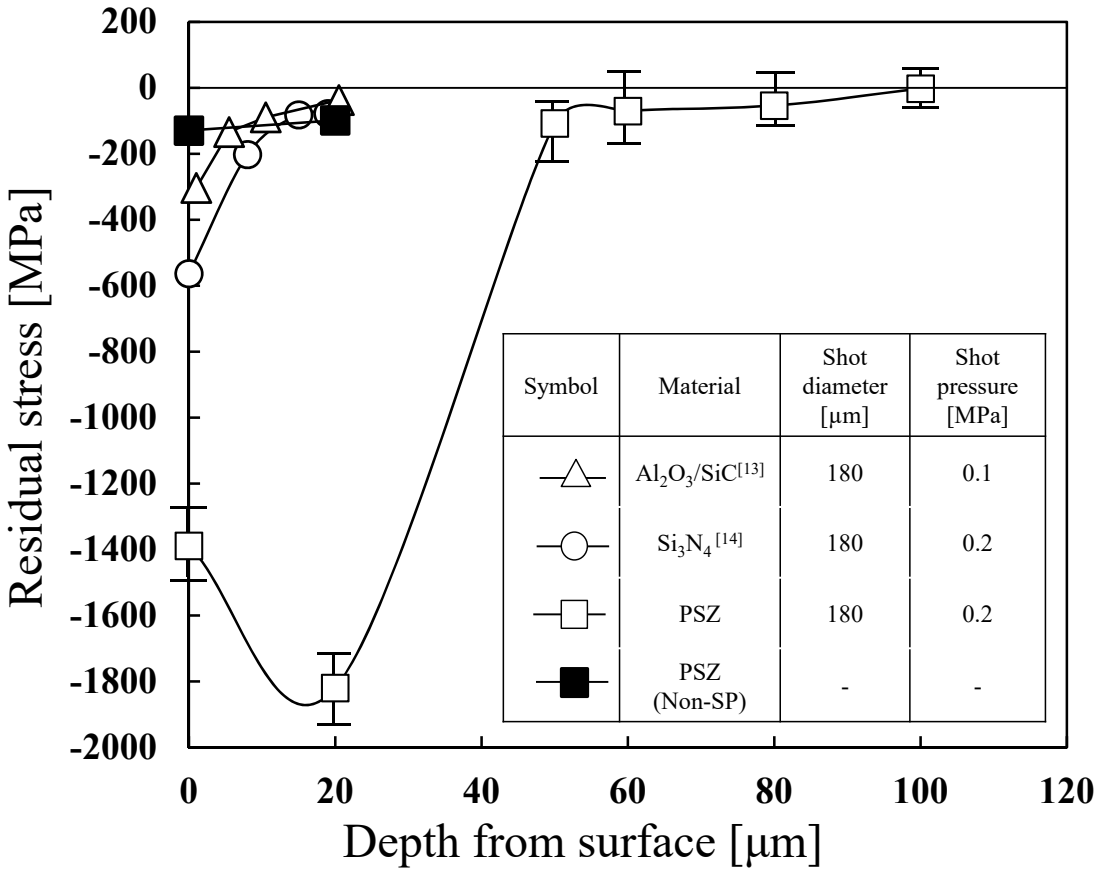

Fig. 2 Relationship between residual stress and depth from surface.

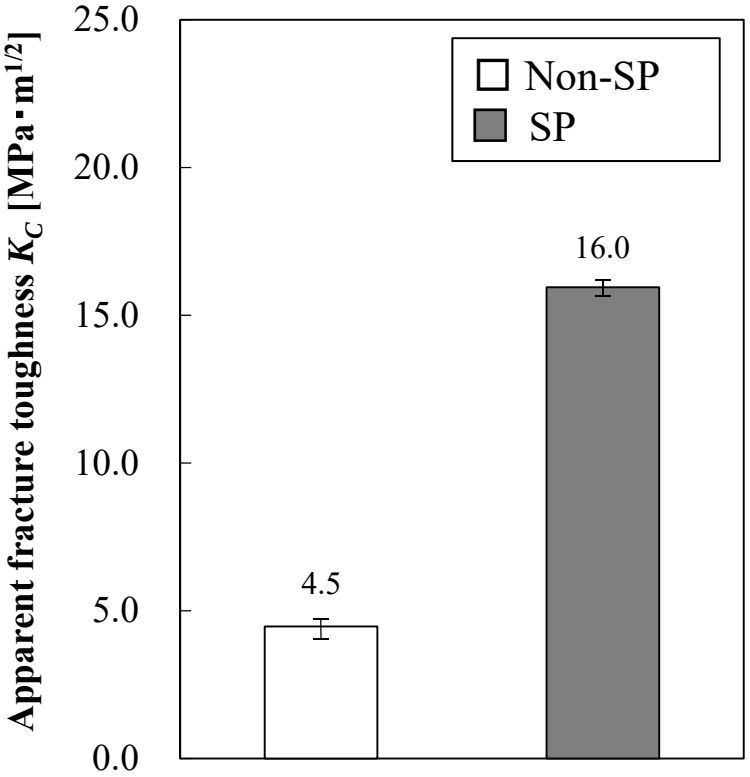

Fig. 3 K_C values of the different surface-treatment specimens. The error bar indicates standard deviation.

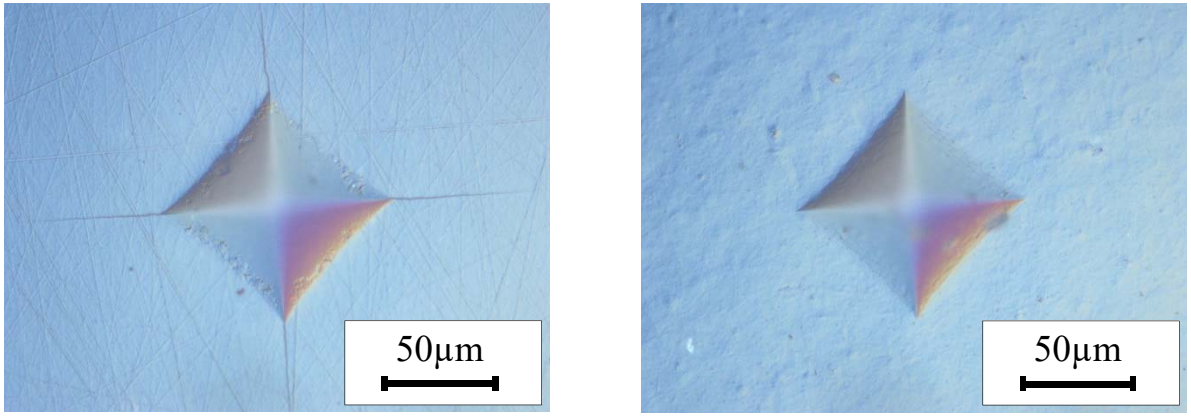

(a) (b)

Fig. 4 Photograph of Vickers indentations and cracks in the (a) Non-SP and (b) SP specimens.

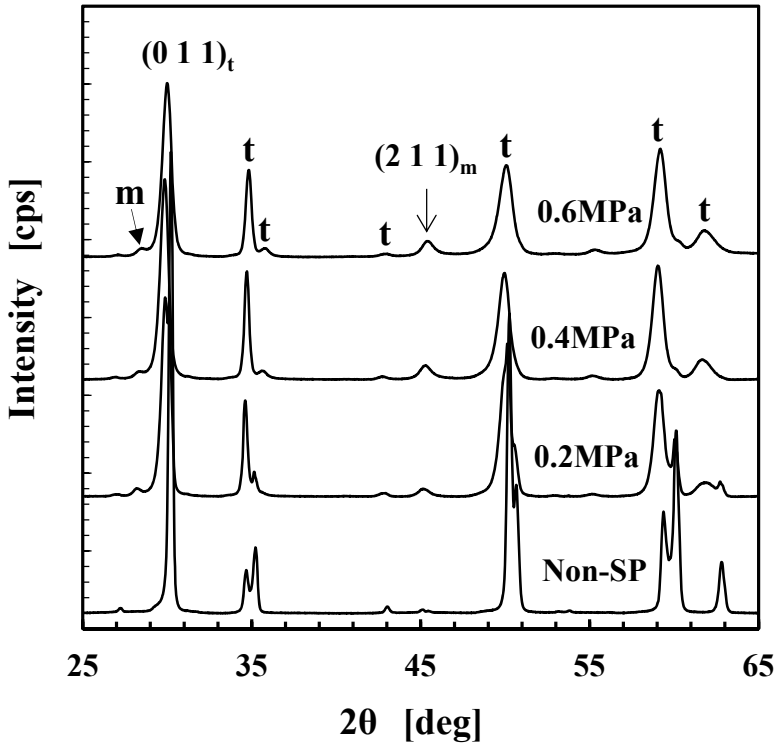

Fig. 5 XRD pattern of the surface of a peened PSZ specimens.

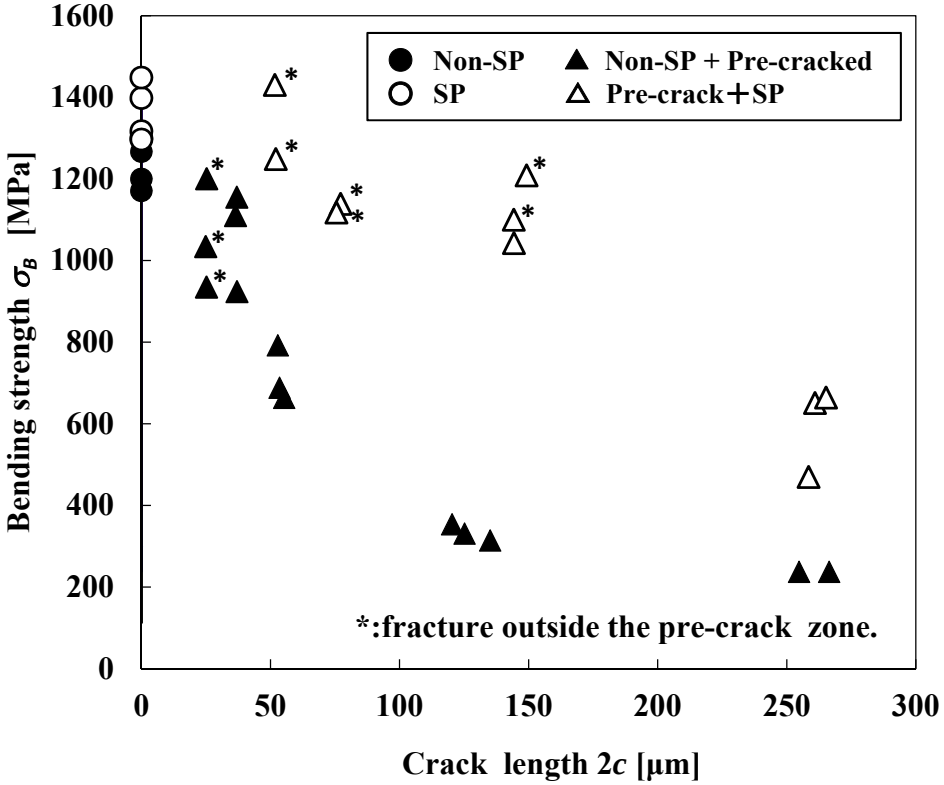

Fig. 6 Relationship between bending strength and crack length.

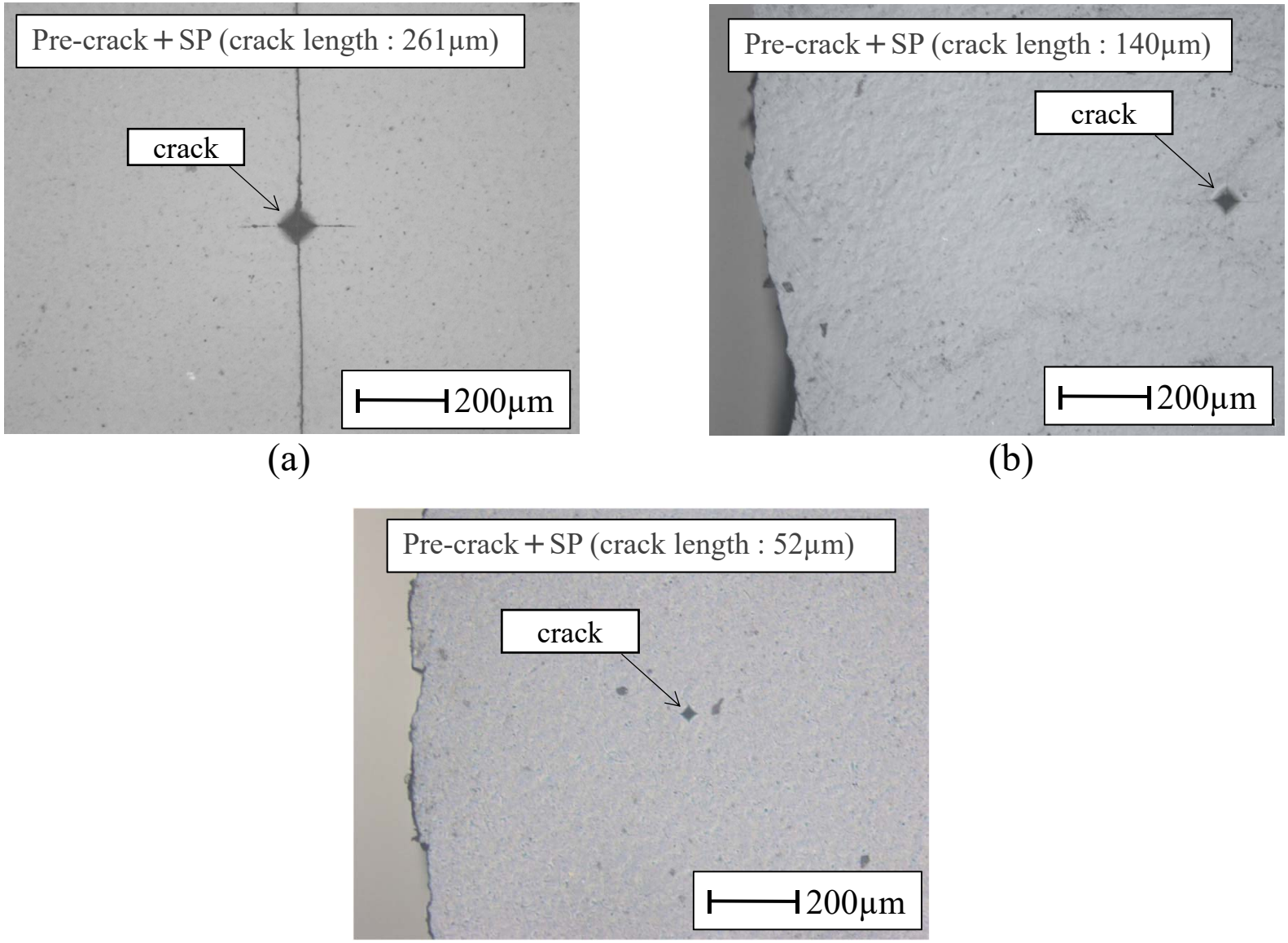

Fig. 7 Surface of Pre-crack+SP specimens after the bending test; bending strengths and crack lengths of (a) σ_B =651 MPa and $2c$ = 261 μm, (b) σ_B =1100 MPa and $2c$ = 140 μm, and (c) σ_B =1431 MPa and $2c$ = 52 μm.

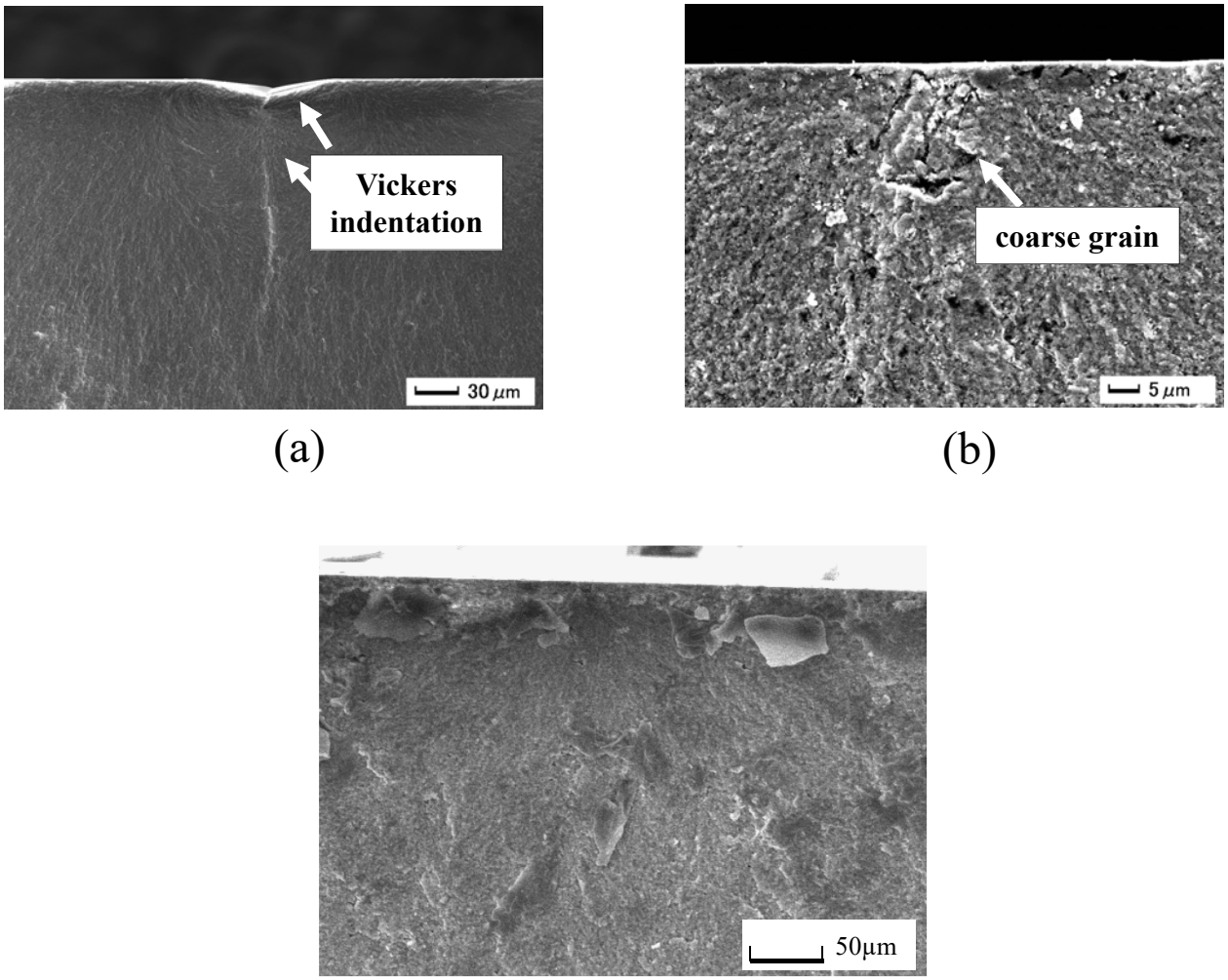

Fig. 8 SEM images showing the origins of fractures: (a) Pre-cracked specimen, 2c = 120 μm, σ_B =354 MPa, (b) Pre-crack+SP specimens, 2c = 140 μm, σ_B =1100 MPa, and (c) Pre-crack+SP specimens, 2c = 51 μm, σ_B =1250 MPa.